# Isotropic Non-Heisenberg Behavior in M-3(dpa)(4)Cl-2 Extended Metal Atom Chains

**ARTICLE** *in* THE JOURNAL OF PHYSICAL CHEMISTRY A · OCTOBER 2010

Impact Factor: 2.69 · DOI: 10.1021/jp106038w · Source: PubMed

# Isotropic Non-Heisenberg Behavior in $M_3(dpa)_4Cl_2$ Extended Metal Atom Chains

**Zahra Tabookht,[†] Xavier López,*[,†] Marc Bénard,[‡] and Coen de Graaf[†,§]**

*Departament de Química Física i Inorgànica, Universitat Rovira i Virgili, C/Marcel.lí Domingo, s/n, 43007, Tarragona, Spain, Laboratoire de Chimie Quantique, Institut de Chimie, LC3-UMR 7177, CNRS-ULP, Strasbourg, France, and Institució Catalana de Recerca i Estudis Avançats (ICREA), Passeig Lluís Company, 23, 08010 Barcelona, Spain*

*Received: June 30, 2010; Revised Manuscript Received: September 20, 2010*

Isotropic deviations to the standard Heisenberg Hamiltonian have been extracted for a series of trinuclear extended metal atom chain complexes, namely, $[Ni_3(dpa)_4Cl_2]$, and the hypothetical $[NiPdNi(dpa)_4Cl_2]$ and $[Pd_3(dpa)_4Cl_2]$, following a scheme recently proposed by Labéguerie and co-workers (*J. Chem. Phys* **2008**, *129*, 154110) within the density functional theory framework. Energy calculations of broken symmetry monodeterminantal solutions of intermediate $M_{s,tot.}$ values can provide an estimate of the magnitude of the biquadratic exchange interaction ($\lambda$) that accounts for these deviations in systems with $S = 1$ magnetic sites. With the B3LYP functional, we obtain $\lambda = 1.37$, 13.8, and 498 $cm^{-1}$ for the three molecules, respectively, meaning that a simple Heisenberg Hamiltonian is enough for describing the magnetic behavior of the $Ni_3$ complex but definitely not for $Pd_3$. In the latter case, the origin of such extreme deviation arises from (i) an energetically affordable local non-Hund state (small intrasite exchange integral, $K \sim 1960$ $cm^{-1}$) and (ii) a very effective overlap between Pd-4d orbitals and a large $J$. Furthermore, this procedure enables us to determine the relative weights of the two types of magnetic interactions, $\sigma$- and $\delta$-like, that contribute to the total magnetic exchange ($J = J_\sigma + J_\delta$). In all of the systems, $J$ is governed by the $\sigma$ interaction by 95−98%.

## Introduction

Magnetic interactions are usually described by the phenomenological Heisenberg−Dirac−van Vleck Hamiltonian,[1,2] which contains the bilinear exchange integral $J_{ij}$ accounting for the magnetic coupling between centers $i$ and $j$:

$$H = \sum_{i<j} J_{ij} S_i S_j \qquad (1)$$

If the magnetic behavior of a molecule can be properly fitted to eq 1, it can be considered as an isotropic Heisenberg system. The application of this Hamiltonian to compounds with high spin moments is done routinely, although it should be performed with care, since the electronic nature of magnetic centers may affect the applicability of this simple spin Hamiltonian. For this reason, in some cases, a more general form of the spin Hamiltonian must be applied to account for deviations to the Heisenberg behavior for compounds with local $S > 1/2$. What are the principal sources of deviation? For $S = 1$ systems,[3] the model space of the Heisenberg Hamiltonian is spanned by the linear combinations of products of the local ground-state spin functions of each magnetic center, i.e., the local triplets. It has been pointed out that the existence of low-lying atomic non-Hund states (local singlet excited states) can be important in some cases.[4] The interaction of these excited states with the model space configurations can lead to deviations from the regular Landé pattern. These so-called isotropic deviations contrast with the anisotropic deviations to the standard magnetic behavior. The latter find their origin in spin−orbit interactions of the unpaired electrons and lead to a zero-field splitting of the different $M_{s,tot.}$ components of the spin functions ($M_{s,tot.}$ being the sum of local $M_s$ values) even in the absence of an external magnetic field. In the herein studied complexes, these effects are not considered since they are expected to be small. The $S = 1$ magnetic centers have a nearly octahedral coordination, and the zero-field splitting is strictly zero in perfect octahedral symmetry. Anyhow, anisotropic effects do not influence the extraction of the isotropic interactions. The complexes studied here are in the strong-exchange limit (as shown below), implying that there is no appreciable spin−orbit interaction between the fundamental quintet, triplet, and singlet states. In these cases, the isotropic part of the interactions can be determined independently of the anisotropic part.[5,6] To prove that the systems we are dealing with in the present work are indeed in the strong exchange limit, we performed a preliminary calculation on the single-ion anisotropy of the $Ni^{2+}$ ion in $[Ni_2(napy)_4Cl_2]^{2+}$. Following the computational strategy outlined in ref 6, the isotropic interaction was found to be about 20 times larger than the single-ion anisotropy.

Considering a system with two magnetic centers of $S = 1$ spin moment each, there are three different electronic configurations that should be taken into account to obtain an accurate first-order description of the magnetic coupling. In the first place, there are the so-called neutral determinants. The magnetic centers stay in their formal oxidation state, and the local triplet coupling of the unpaired electrons is maintained. The local triplets can be coupled to singlet, triplet, and quintet states. In the second place, one should consider the ionic determinants in which one electron is transferred from site $i$ to site $j$ or vice versa. The ionic determinants largely enhance the magnetic coupling but do not lead to deviations of the standard magnetic behavior. Finally, for the non-Hund states the number of

* To whom correspondence should be addressed. E-mail: javier.lopez@urv.cat.
[†] Universitat Rovira i Virgili.
[‡] CNRS-ULP.
[§] ICREA.

10.1021/jp106038w 
Published on Web 10/28/2010

electrons per magnetic site remains as in the neutral determinants, but the local triplet coupling is changed to singlet on one (or both) site(s). These non-Hund states interact in a nonuniform manner with the states contained in the Heisenberg model space.[4] The coupling of the ionic and the neutral configurations is essential in the description of the magnetic interactions and is usually identified as a hopping integral $t$, as described by the Hubbard Hamiltonian.[7] The energy of the ionic configuration with respect to the neutral one is $U$. The magnetic coupling constant depends on these two parameters through the second-order perturbative expression $J \propto -t^2/U$. The hopping integral between centers $i$ and $j$ strongly depends on the nature of the orbitals involved in such a process. In the present case, as will be discussed later, there are two possible hopping integrals ($t_\sigma$ and $t_\delta$), which relate to two different magnetic interaction paths denoted by $J_\sigma$ and $J_\delta$.

In a series of recent works, Guihéry and collaborators have developed,[4,8,9] explained, and tested[10] a more general form for the spin Hamiltonian that can be applied to $S = 1$ compounds. The spin Hamiltonian, called non-Heisenberg in short from now on, contains the well-known biquadratic interaction (second term) and a three-body operator (third term):

$$H = \sum_{\langle i,j \rangle} J_{ij}^{\text{eff}} S_i S_j + \lambda_{i,j} (S_i S_j)^2 + \sum_{i,\langle j,k \rangle} \frac{B_{ji} B_{ik}}{2K} [(S_i S_j)(S_i S_k) + (S_i S_k)(S_i S_j) - (S_i S_i)(S_j S_k)] \quad (2)$$

These additional interactions arise from contributions of the locally excited states (non-Hund states) to the $N$-electron wave function. The three-body interaction was found to be as important as the biquadratic exchange interactions in the magnetic coupling between $Ni^{2+}$ ions along a linear Ni−O−Ni−O−Ni exchange path.[9]

To the fourth order of perturbation, and with consideration of the local singlets $S^0$ as the only accessible non-Hund states, the magnitude of these interactions can be obtained from eqs 3−6, where $(t_\sigma)_{ij}$ is the hopping integral between two $\sigma$ orbitals and $(t_\delta)_{ij}$ is the hopping integral between two $\delta$ orbitals. $U$ and $K$ are the on-site repulsion integral and intrasite exchange integral, respectively:

$$J_{ij} = \frac{(t_\sigma)_{ij}^2}{U} + \frac{(t_\delta)_{ij}^2}{U} \quad (3)$$

$$B_{ij} = \frac{(t_\sigma)_{ij}^2}{U} - \frac{(t_\delta)_{ij}^2}{U} \quad (4)$$

$$J_{\text{eff}} = \frac{(t_\sigma)_{ij}^2}{U} + \frac{(t_\delta)_{ij}^2}{U} + \frac{B_{ij}^2}{K} = J_{ij} + \frac{B_{ij}^2}{K} \quad (5)$$

$$\lambda_{ij} = \frac{B_{ij}^2}{K} - \frac{J_{ij}^2}{4K} \quad (6)$$

Extended metal atom chains (EMACs) form an interesting family of compounds potentially suitable for being applicable as conducting nanowires or switches or by their magnetic properties.[11−23] They consist of a linear backbone of transition metal atoms (M) surrounded by a group of organic ligands (L). A classification has been proposed, depending on how they are built up, in *supported* and *unsupported* chain compounds.[11] In the present paper, supported nanowires are studied, where purposely designed ligands (the poly(pyridylamide) family being the most typical)[24] keep the metal atoms close to bonding distance in a string conformation. The most common supported EMACs are those with four equatorial and two axial ligands, with general formula $[M_n(L)_4X_2]$, and $3 \le n \le 9$. Among the magnetic systems of this family, all feature antiferromagnetism irrespective of the metal atoms present in the chain.

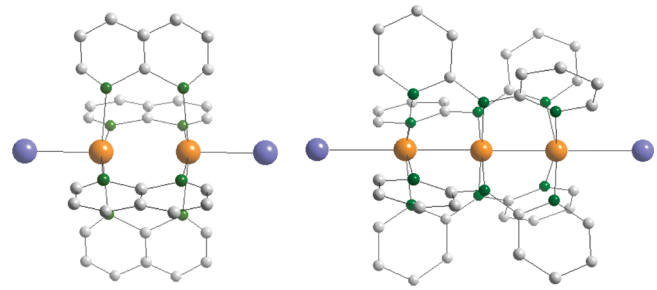

**Figure 1.** Bimetallic $[Ni_2(napy)_4Cl_2]^{2+}$ model system (left) and the trimetallic $[M_3(dpa)_4Cl_2]$ EMAC. Color-coding: orange, metal; green, nitrogen; blue, chlorine; light gray, carbon. Hydrogen atoms are not drawn for clarity.

We herein deal with $n = 3$ homo- and heterometallic symmetric systems, $[Ni_3(dpa)_4Cl_2]$, $[NiPdNi(dpa)_4Cl_2]$, and $[Pd_3(dpa)_4Cl_2]$ (dpa = dipyridylamide). The central metal atom is diamagnetic, and each terminal metal is paramagnetic with $S = 1$. Thus, four unpaired electrons interact; two of them occupy $\sigma$-type orbitals, and the other two are in $\delta$-type orbitals. Our purpose is to gain some more insight into the magnetic properties of such EMACs by means of density functional theory (DFT) calculations. The main goals of the present work are as follows: (i) to establish the importance of the terms that introduce deviations to the standard Heisenberg Hamiltonian in compounds with $S = 1$ centers, (ii) to compute the magnetic parameters of the general form of spin Hamiltonian in eq 2, and (iii) to determine the relative contribution of the $\sigma$- and $\delta$-type interactions to the total magnetic coupling. In this study we also tackle a smaller bimetallic Ni model compound, $[Ni_2(napy)_4Cl_2]^{2+}$ (napy = naphtyridine), to check the validity of the DFT results against the more accurate difference dedicated configuration interaction (DDCI) method[25,26] (see Computational Information for a detailed description of the methods). Figure 1 shows the structure of bi- and trimetallic systems.

## DFT-KS Description of the Magnetic Interaction between Two $S = 1$ Centers

DDCI is considered one of the most accurate computational methods to obtain magnetic coupling constants. The method has been applied to many systems ever since its introduction in 1992. In general, DDCI estimates are in good agreement with experimental data; see, for example, refs 27−29 among many others. The method is, however, computationally expensive and virtually impossible to apply for medium- and large-sized systems. Reasonably accurate and computationally less expensive solutions are achieved by means of the DFT. In this methodology, the most widely used Kohn−Sham (KS) version is based on a monodeterminantal assumption, which is the main limitation of this methodology. This implies that, for spin-coupled open-shell systems (such as magnetic systems), the DFT accuracy is severely limited. However, this shortcoming can be pragmatically bypassed with the broken symmetry approach, which provides helpful solutions and has amply shown its

**TABLE 1: Monodeterminantal Solutions and Associated Second-Order Perturbative Energy Expressions for $M_{s,tot.} = 2$, 1, and 0**

| $M_{s,tot.}$ | configuration | atom 1 | atom 2 | $E^{(2)}$ [a] |
|---|---|---|---|---|
| 2 | $D^1D^1$ | $\lvert\sigma_1\delta_1\rvert$ | $\lvert\sigma_2\delta_2\rvert$ | $-2K$ |
| 0 | $D^1D^{-1}$ | $\lvert\sigma_1\delta_1\rvert$ | $\lvert\bar{\sigma}_2\bar{\delta}_2\rvert$ | $-2K - 2\frac{(t_\sigma)^2}{U} - 2\frac{(t_\delta)^2}{U}$ |
| 1 | $D^1D^0$ | $\lvert\sigma_1\delta_1\rvert$ | $\lvert\bar{\sigma}_2\delta_2\rvert$ | $-K - 2\frac{(t_\sigma)^2}{U}$ |
| 0 | $D^0D^0$ | $\lvert\sigma_1\bar{\delta}_1\rvert$ | $\lvert\bar{\sigma}_2\delta_2\rvert$ | $-2\frac{(t_\sigma)^2}{U} - 2\frac{(t_\delta)^2}{U}$ |
| 0 | closed shell | $\lvert\sigma_g\bar{\sigma}_g\delta_g\bar{\delta}_g\rvert$ | | $2(t_\sigma + t_\delta) + U$ |

[a] The denominators in the energy expressions have been simplified from $(U - K)$ to $U$ under the assumption $U \gg K$ throughout this work. See ref 10 for details.

usefulness in the description of isotropic Heisenberg systems.[30−37] A strategy that goes beyond the usual broken symmetry approximation and gives access to non-Heisenberg terms was reported by Malrieu and colleagues.[10] They have used the other broken symmetry solutions of intermediate values of $M_{s,tot.}$, as well as $M_{s,tot.}^{max} = 2$ and $M_{s,tot.}^{min} = 0$, combined with a closed-shell solution.[38] We denote $D^{M_s}$ an atomic determinant with a given $M_s$ value. Within this notation, the previous solutions can be written as $D^1D^1$ and $D^1D^{-1}$ (or $D^{-1}D^1$), respectively. The other neutral monodeterminantal solutions are as follows: $D^0D^1$ and $D^1D^0$ for $M_s = 1$, and $D^0D^0$ for $M_s = 0$. At the zero order of perturbation, the energies $E^{(0)}$ of all solutions arise from the intrasite exchange integral $K$, which always favors the maximal local $M_s$. $E^{(0)} = -2K$ for $D^1D^1$, $D^1D^{-1}$, and $D^{-1}D^1$). For $D^0D^1$ (or $D^1D^0$) and $D^0D^0$, the energies are $-K$ and 0, respectively. The ionic configurations that are treated at the second order of perturbation in the Heisenberg Hamiltonian incorporate the kinetic exchange contributions to the zero-order energies. The energy expression of each solution at the second order of perturbation, $E^{(2)}$, is shown in Table 1. Each magnetic center contains one $\sigma$ and one $\delta$ localized orbital. The energy obtained for different determinants by broken symmetry approach providing the $U$ and $t$ parameters are connected by eqs 3−6 to the $J$, $\lambda$, $K$, and $B$ Heisenberg values. The closed shell determinant must also be considered for a complete determination of the parameters.[10]

The most stable solution in antiferromagnetic systems is $D^1D^{-1}$, corresponding to an open-shell with $M_s = 0$, followed by the $M_{s,tot.} = 2$ determinant $D^1D^1$. These two solutions are based on local Hund states. Determinants $D^1D^0$ and $D^0D^0$ are products of local non-Hund states and, hence, much higher in energy. The closed-shell configuration $\lvert\sigma_g\bar{\sigma}_g\delta_g\bar{\delta}_g\rvert$ is the highest one.

## Computational Information

Geometry optimizations and energy calculations in this work have been performed with the DFT methodology using the B3LYP hybrid exchange-correlation functional (20% exact Fock exchange) implemented in the GAUSSIAN 03 package.[39] Variations in the percent of exact Fock exchange have been utilized where indicated. The PBE0 functional[40] has also been applied for a comparative issue. Geometry optimizations were carried out for the hypothetical trimetallic complexes $[NiPdNi(dpa)_4Cl_2]$ and $[Pd_3(dpa)_4Cl_2]$, and for the model system $[Ni_2(napy)_4Cl_2]^{2+}$ in their ground states, whereas $[Ni_3(dpa)_4Cl_2]$ has been studied with a symmetrized geometry containing the Ni−Ni, Ni−N, and Ni−Cl experimental distances.[41] Concerning

**TABLE 2: Selected Interatomic Distances[a] for $[Ni_2(napy)_4Cl_2]^{2+}$, $[Ni_3(dpa)_4Cl_2]$, $[NiPdNi(dpa)_4Cl_2]$, and $[Pd_3(dpa)_4Cl_2]$**

| | $Ni_2$[c] | $Ni_3$[b] | NiPdNi[c] | $Pd_3$[c] |
|---|---|---|---|---|
| M−M | 2.912 | 2.43 | 2.513 | 2.544 |
| M−Cl | 1.856 | 2.33 | 2.398 | 2.564 |
| $M-N_{term}$ | 1.995 | 2.09 | 2.162 | 2.258 |
| $M-N_{cent}$ | | 1.89 | 2.040 | 2.062 |

[a] Values in angstroms. [b] Mean values taken from the experimental geometry reported in ref 12. [c] DFT optimized geometries (see Computational Information for procedure).

$[Ni_2(napy)_4Cl_2]^{2+}$, a Ni−Ni distance of 2.912 Å has been assumed for reasons discussed below, and the rest of the molecular geometry has been optimized. Table 2 shows some important geometrical parameters for the mentioned molecules. For the other electronic configurations studied, single-point energy calculations were performed at the geometry of the ground state. We used the unrestricted formalism for all the open shell configurations. All-electron valence double-$\zeta$ basis sets (D95 V) were used to describe C and H atoms, and a full double-$\zeta$ (D95) basis set supplemented with one d polarization function for N and a double-$\zeta$ (LANL2DZ basis) for Cl. For the metal atoms, the valence shells were described with LANL2DZ basis supplemented with one *f*-type polarization function with exponent 3.13 for Ni and 1.472 for Pd. For the heavy atoms (Cl, Ni, and Pd), the core electrons were modeled with a Los Alamos core potential.

For $[Ni_2(napy)_4Cl_2]^{2+}$, DDCI calculations were carried out to check the validity of the DFT procedure to address the deviations to the Heisenberg Hamiltonian. The DDCI expansion of the wave function includes all single and double replacements from a complete active space self-consistent field (CASSCF) reference wave function, excluding the double replacements from inactive to virtual orbitals. These configurations contribute in quasi-degenerate second-order perturbation theory equally to the energy of the different states and, hence, can be omitted for the calculation of vertical energy differences.[42] The active space in the CASSCF calculation contains the four magnetic orbitals with mainly Ni-3d character and the four unpaired electrons present in the molecule. The CASSCF calculations have been performed with the MOLCAS 7 package.[43] The one-electron basis used to expand the MOs is of the atomic natural orbital type for all atoms. We have employed ANO-RCC type for Ni atoms (5s, 4p, 3d), for the bridging N atoms (3s, 2p), and for axial Cl ligands (4s, 3p). For C and H atoms, we used (3s, 2p) and (2s) basis sets, respectively.[44]

The DDCI formalism requires the use of a common set of orbitals for the states of interest. Therefore, average natural orbitals have been constructed by diagonalizing the average of the singlet, triplet, and quintet CASSCF density matrices. To reduce the computational cost of the DDCI calculation, these average MOs were transformed to so-called dedicated orbitals.[45] This unitary transformation consists of a block diagonalization of the inactive and virtual part of the DDCI2 difference density matrix $\rho_{diff} = (2\rho_Q - \rho_T - \rho_S)$, where Q, T, and S stand for quintet, triplet and singlet, respectively. The resulting dedicated orbitals are ordered by increasing relevance to the energy difference between the states, and the less relevant orbitals were not used in the generation of the CI expansion. It has been shown that this procedure reproduces the DDCI results obtained with the full MO space at a much lower computational cost.[45,46] The maximum number of dedicated orbitals that we managed to include in DDCI calculations was 217 over a total of 349

**TABLE 3: DFT-Based Electronic and Magnetic Interaction Values[a] for $[Ni_2(napy)_4Cl_2]^{2+}$**

| | | | | | |
|---|---|---|---|---|---|
| $K$ | 4057 | $U$ | 27 131 | % $J_\sigma$ | 83.2 |
| $t_\delta$ | −1540 | $J_\delta$ | 87.9 | $J$ | 520 |
| $t_\sigma$ | −3428 | $J_\sigma$ | 433 | $J_{eff}$ | 550 |
| $B$ | 345 | % $J_\delta$ | 16.8 | $\lambda$ | 12.7 |

[a] In $cm^{-1}$.

molecular orbitals. As will be shown below, this number of MOs is enough to converge to the DDCI result of the complete MO space. DDCI calculations have been performed with the CASDI chain.[47]

## Results

**A. $[Ni_2(napy)_4Cl_2]^{2+}$ Model System ($Ni_2$).** In the first part of the study we present a model system with the following characteristics: (1) it contains two $S = 1$ magnetic centers (Ni atoms), (2) the ligands are as similar as possible to the dpa ligand of real EMACs to make the magnetic coupling comparable, and (3) it is smaller than the 89-atom $M_3(dpa)_4Cl_2$ nanowires. We found that a napy-based molecule accomplishes this list fairly well, although it cannot be considered to be really small for DDCI standards. However, smaller ligands that could mimic the role of poly(pyridylamides) in EMACS are rather crude models since the pyridine rings are mandatory to reproduce (i) the correct difference of basicities between the two types of nitrogen donors and (ii) the flexibility of the ligand molecules, and more specifically the characteristic twist of dpa and related molecules around the metal chain. The geometry of the $[Ni_2(napy)_4Cl_2]^{2+}$ model system was optimized with DFT, getting to a structure with a $\sigma$ covalent Ni−Ni bond. Since we needed four unpaired electrons to deal with $S = 1$ magnetic centers, such $\sigma$ bond is inadequate and must be removed. To this end, we performed a Ni−Ni distance scan, where at each step the rest of the molecule was optimized. We found an electronic structure convenient for our goal at 2.912 Å (significantly longer than the equilibrium distance at the B3LYP level).

***1. DFT Calculations.*** We have computed the energy of the solutions listed in Table 1. It is important to note that the $\{\sigma_1, \sigma_2, \delta_1, \delta_2\}$ set of localized orbitals are not exactly the same in all the solutions considered since the process of convergence of each broken symmetry solution has produced new orbitals adapted to the particular spin orientations. That is, each broken symmetry solution contains a particular degree of electron delocalization and thus a slightly different amount of ionic character. Specifically, the ionic contribution is strictly zero in the quintet determinant. For simplicity, we have used the same orbital labeling for all the local magnetic orbitals present in the determinants.

Using the second-order perturbative energy expressions of Table 1 in combination with eqs 3−6, one can obtain the parameters shown in Table 3. The corresponding $J_{eff} = 550$ $cm^{-1}$ is very large, as expected, since it arises from the coupling between two neighboring $S = 1$ nickel atoms instead of the next-nearest interaction of the typical $Ni_3$ EMAC. The relative magnitude of $t_\sigma$ and $t_\delta$ reveals that the electron hopping is much more effective within the $\sigma$ orbitals, representing a $\sigma$-like dominating magnetic exchange (~80% of total $J_{eff}$). The calculated $\lambda = 12.7$ $cm^{-1}$, to be compared to the effective coupling, $J_{eff} = 550$ $cm^{-1}$, is quite large in comparison with previously reported deviations.[4,8]

***2. DDCI Calculations.*** It is well-known that the most accurate description of highly correlated magnetic systems can be obtained by ab initio methods. In particular, the DDCI method has best performed in not too large magnetic systems.[25,26,48] To perform the DDCI runs, we used the same geometries as those for DFT energy calculations. The magnetic parameters related to non-Heisenberg terms obtained with DDCI are based on the minimal CAS(4,4). This set of orbitals is composed of two linear combinations of $\delta$ character and two of $\sigma$ character, shown in Figure 2.

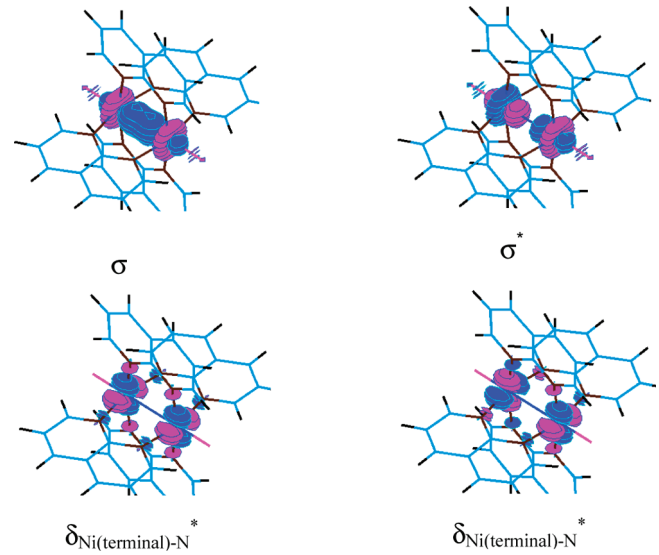


**Figure 2.** Symmetry-adapted orbitals of the CAS(4,4) for the $Ni_2$ model system. Two are $\sigma$-like, and the other two are $\delta$-like.

**TABLE 4: Magnetic Interaction Parameters[a] at Different Approximations to the Exact *N*-Electron Wave Function**

| | $J_1$ | $J_2$ | $\lambda = J_2 - J_1$ |
|---|---|---|---|
| CAS(4,4) | 129 | 122 | −6.77 |
| DDCI2 | 438 | 458 | 20.0 |
| DDCI(38)[b] | 356 | 369 | 13.0 |
| DDCI(87) | 365 | 381 | 15.5 |
| DDCI(203) | 370 | 393 | 23.1 |
| DDCI(217) | 366 | 392 | 26.5 |

[a] In $cm^{-1}$. [b] In parentheses, number of dedicated orbitals in the DDCI run.

To extract the magnitude of the biquadratic term from the non-Heisenberg Hamiltonian, eq 2, we have calculated $J_1$, $J_2$, and $\lambda$ using eqs 7−9. $E$(S), $E$(T), and $E$(Q) indicate the energy of singlet, triplet, and quintet states, respectively.[8]

$$J_1 = \frac{E(S) - E(Q)}{3} \quad (7)$$

$$J_2 = \frac{E(T) - E(Q)}{2} \quad (8)$$

$$\lambda = J_2 - J_1 \quad (9)$$

At this point, we are interested in comparing the DFT and DDCI values of $J$ and $\lambda$ to validate the DFT method. The DDCI values of $J_1$ and $J_2$ hardly depend on the number of dedicated orbitals included, as observed in Table 4. We can thus take the DDCI results as accurate enough and a benchmark for the rest of the discussions. From the whole series of DDCI calculations (38−217 dedicated orbitals), the values of $J_1$ and $J_2$ tend to converge to ~366 and ~392 $cm^{-1}$, respectively. Also, $\lambda$ gets larger when more dedicated orbitals are considered as the

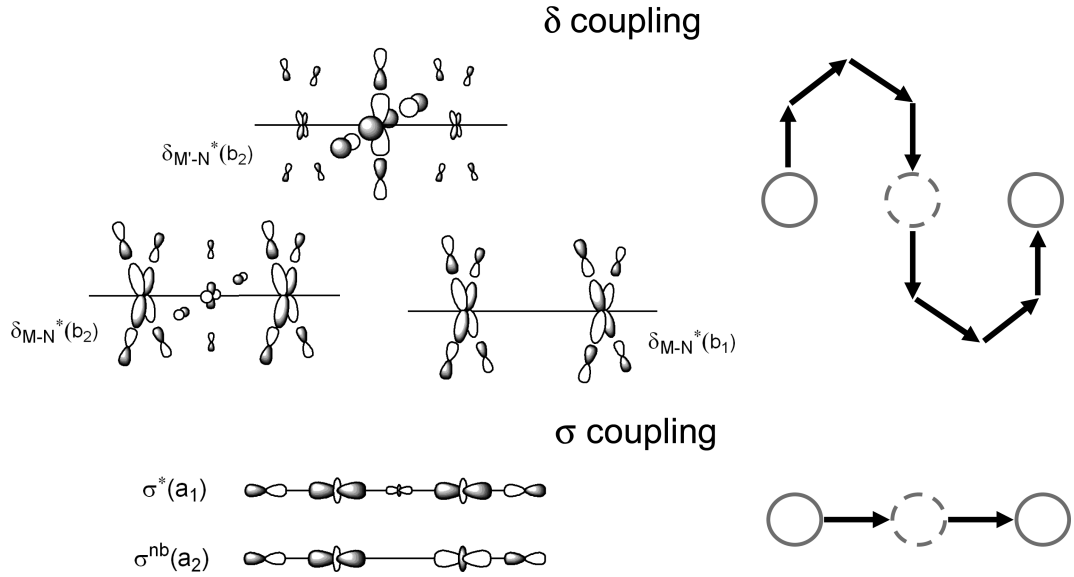


**Figure 3.** Molecular orbitals involved in the $\delta$ and $\sigma$ types of magnetic coupling in EMACs with $S = 1$ centers, and schematic view of the two coupling pathways: through dpa ligands (top) and through central nickel (bottom).

difference between $J_1$ and $J_2$ increases. For DDCI(217) $\lambda = 26.5$ cm$^{-1}$, a rather large value and our *best* estimate for the $Ni_2$ model system. Comparing Tables 3 and 4, it can be seen at a qualitative level that the $J$ and $\lambda$ parameters are, in general, comparable for DDCI and DFT methods, although the B3LYP functional overestimates, as expected, the values of $J$. In this particular case, the best coincidence of $J$ between the two methodologies would occur at a higher percentage of Fock exchange than the one herein considered. This behavior has also been found in other systems,[10] but this cannot be taken as a general fact.

Here, we come shortly back to the question of the magnetic anisotropy in the compounds studied here. To demonstrate the assumption that the complexes are in the strong exchange limit, we calculated the single-ion anisotropy of the $Ni^{2+}$ ion in the $Ni_2$ model complex. For this purpose, we followed the strategy described in ref 6. The calculated single-ion anisotropy is less than 20 cm$^{-1}$, which is about 20 times smaller than the estimated isotropic exchange, confirming the complex to be in the strong exchange limit, and, consequently, no interference of the anisotropy and the isotropic interactions.

**B. $[Ni_3(dpa)_4Cl_2]$ System ($Ni_3$).** The DFT strategy used for the $Ni_2$ model system to compute the deviation from the Heisenberg behavior is now applied to trinuclear EMAC systems. We are also interested in the quantitative determination of the relative contributions to the total magnetic coupling ($J$) originating in each coupling pathway, namely, those involving the $\delta$ and $\sigma$ orbitals (Figure 3). This particular issue has been already introduced in previous publications,[49] although not quantified until now. The $Ni_3$ compound appears as a good candidate for such a study since it has been synthesized and structurally characterized,[50] and its magnetic properties have been previously studied, both with experiment and by means of standard, DFT-based broken symmetry calculations.[12,13,51,52]

The experimental temperature dependence of the magnetic susceptibility was fitted with a $J$ value of $\sim$200 cm$^{-1}$ for the coupling between the two external Ni centers.[12,15,52] The previously reported DFT estimate of 91 cm$^{-1}$ quite surprisingly does not show the common DFT overestimation of the antiferromagnetic coupling strength. This cannot be solely attributed to possible deficiencies in the B3LYP functional, since a test calculation with the PBE0 functional at the same geometry gives also an important underestimation resulting in $J = 64$ cm$^{-1}$ (see Table S1 in the Supporting Information for a comparison between the results obtained with the B3LYP and PBE0 functionals on the DFT-optimized and the experimental geometries). One of the factors that contributes to the previously reported underestimation of $J$ is the fact that the B3LYP optimized Ni−Ni distances are slightly too long in comparison with the experimental ones. Applying the experimental structure, with a Ni−Ni distance 0.05 Å shorter than the B3LYP optimized one, we obtain a $J$-value of 112.5 cm$^{-1}$ for B3LYP and 82.3 cm$^{-1}$ for PBE0. Moreover, the coupling also depends on the percentage of HF exchange in the hybrid functional. For instance, reducing this percentage to 10% results in a much larger $J$ of 159 cm$^{-1}$.[51] However, since the main question here is whether its magnetic behavior can be accurately described with the simple $H = JS_1S_2$ Heisenberg Hamiltonian, we do not further discuss the appropriateness of the different functionals but stick to B3LYP using the experimental geometry, which leads to a reasonable estimate of the coupling and was shown to nicely reproduce the deviations to the Heisenberg behavior in the previous section. The origin of the theoretical underestimation of $J$ for Ni-derived complexes such as $[Ni_3(dpa)_4Cl_2]$[51] and $[Ni_5(tpda)_4Cl_2]$[53,54] deserves a separate analysis.[55]

A main goal of the present work is to quantify the relative weights of the $\delta$ and $\sigma$ magnetic coupling paths for the $Ni_3$ molecule. For this purpose, using Malrieu's approach,[10] we obtain the relevant parameters listed in Table 5. The computed values for the electron hopping are $t_\delta = -384$ cm$^{-1}$ and $t_\sigma = -1627$ cm$^{-1}$. As for $Ni_2$, $t_\sigma$ is found to be largely dominant. Consequently, $J_\sigma$ governs the total $J$ due to the more effective hopping integral $t_\sigma$, accounting for 94.7% of the total magnetic coupling in $Ni_3$. The magnitude of $K$ appears similar for the $Ni_3$ and $Ni_2$ model complexes, and also for the $Ni^{2+}$ ion embedded in the $La_2NiO_4$ crystal.[10] This confirms that the intrasite exchange integral is essentially an atomic parameter moderately sensitive to the ligand field. In the present case, the difference between the $K$ values computed for $Ni_2$ ($\sim$4000 cm$^{-1}$) and $Ni_3$ or NiPdNi ($\sim$5000 cm$^{-1}$) can be traced to the different interaction strengths between the magnetic metal atoms and the ligands in both cases, as reflected by the Ni−N distances (Table 2). The formal definition of $U$ as the energy difference between the neutral and the ionic structures could suggest that this

**TABLE 5: Electronic and Magnetic Interaction Parameters[a] for $[M_3(dpa)_4Cl_2]$ Compounds**

| | $Ni_3$ | NiPdNi | $Pd_3$[b] |
|---|---|---|---|
| $K$ | 4984 | 5065 | 1960 |
| $t_\delta$ | −384 | −463 | −1137 |
| $t_\sigma$ | −1627 | −3178 | −4960 |
| $B$ | 98.9 | 310 | 1194 |
| $U$ | 25 292 | 31 954 | 19 590 |
| $J_\delta$ | 5.81 | 6.69 | 66.0 |
| $J_\sigma$ | 104.7 | 316.1 | 1258 |
| % $J_\delta$ | 5.3 | 2.1 | 5.0 |
| % $J_\sigma$ | 94.7 | 97.9 | 95.0 |
| $J$ | 110.5 | 323.4 | 1323 |
| $J_{eff}$ | 112.5 | 342.0 | 2040 |
| $\lambda$ | 1.37 | 13.8 | 498 |

[a] Values in $cm^{-1}$. [b] Parameters obtained with 25% of exact Fock exchange (see text for details).

parameter is not so local as $K$. Nevertheless, the value of $U$ computed for $Ni_3$ (25 292 $cm^{-1}$, Table 5) is very similar to either model complex of $Ni^{2+}$ obtained at the same level of theory (27 131 $cm^{-1}$ for $[Ni_2(napy)_4Cl_2]^{2+}$ and 26 542 $cm^{-1}$ for $La_2NiO_4$ [10]). It however increases by 26% to 31 954 $cm^{-1}$ in the mixed-metal complex NiPdNi. As a first approximation, however, the variation of the magnetic coupling in the various Ni compounds can be primarily attributed to the differences in the hopping parameters.

With the B3LYP functional, the percent deviation from the Heisenberg Hamiltonian calculated for the $Ni_3$ complex is modest: $[(J_{eff} - J)/J_{eff}] \times 100 = 1.8\%$, validating the experimental extraction of the magnetic interactions through the simple Heisenberg Hamiltonian. Considering now the criterion $\lambda_{ij}$ defined in eqs 3−6, we have to consider for $Ni_3$ the case where the $\sigma$ coupling is largely dominant (94.7%), which means that $B$ and $J$ have the same order of magnitude, and $\lambda$ can be approached by the positive term $B^2/K$ alone, which is $(t_\sigma)^4/KU^2$. This term remains negligible due to the small value of $B$ combined with large values of $U$ and $K$, from which it can be inferred that the validity of the Heisenberg Hamiltonian in this case is due to the $\sigma$ coupling remaining relatively weak, although largely dominant. In the case of $Ni_2$, $t_\sigma$ is more than twice as large with similar values of $U$ and $K$. Even though a more important contribution from $J_\delta$ (16.8%, Table 3) limits the increase of $\lambda$, the validity criterion is nevertheless raised to 12.7 $cm^{-1}$ for $Ni_2$, compared to only 1.37 $cm^{-1}$ for $Ni_3$.

It was reported by some of us in the past[51] that trinuclear EMAC complexes, such as $Ni_3(dpa)_4Cl_2$, can feature the so-called 4-electron/3-center $\sigma$ bond. It arises from a $(\sigma)^2(\sigma^{nb})^1(\sigma^*)^1$ configuration. This special situation can usually be associated to computational artifacts[56,57] if a density functional not correcting the self-interaction error (SIE) is used. One consequence of the SIE is that the absolute orbital energies are shifted to unrealistic values that, for some chemical analysis, should be corrected. It is worth pointing out here that its implications in our study are secondary and they do not affect the general conclusions extracted. The fact that we use rather small energy differences associated with very similar electron density distributions in some way minimizes the effect of the SIE. Development of new functionals correcting the SIE is in continuous progress.[58,59]

**C. Hypothetical $[Pd_3(dpa)_4Cl_2]$ ($Pd_3$) and $[NiPdNi(dpa)_4Cl_2]$ (NiPdNi) Systems.** $Pd_3$ and NiPdNi complexes were theoretically studied by some of us quite recently.[60] In spite of being hypothetical compounds, they can provide us with valuable results concerning the change induced in some magnetic properties by the replacement of one or several metal atoms by heavier homologues and the associated deviation to the Heisenberg behavior. It is also interesting to extend the analysis of the $\sigma$ and $\delta$ contributions to $J$ in these derivatives. The set of parameters defined in eqs 3−6 was therefore computed for these two complexes.

***1. NiPdNi(dpa)$_4$Cl$_2$.*** The replacement of the central Ni by Pd induces significant changes concerning more specifically the $\sigma$ hopping integral, which is almost doubled, whereas $t_\delta$ remains fairly constant. Therefore, the increase from $J = 110.5$ $cm^{-1}$ to 323.4 $cm^{-1}$ from $Ni_3$ to NiPdNi almost exclusively originates in the $\sigma$ interaction, which now amounts to 97.9% of the total coupling. This increase of the $\sigma$ contribution can be assigned to the well-documented trend of the second row transition metals to favor more delocalized and covalent interactions with their neighbors, in comparison with their first row homologues. The interaction along the $\sigma$ axis is therefore enhanced by a larger overlap between $d(z^2)_{Ni}$ and $d(z^2)_{Pd}$ orbitals, in keeping with the larger energy gap obtained between the $\sigma_{nb}$ and $\sigma^*$ orbitals. The $\delta$ interaction, which relies only for a small part on a direct overlap between metal orbitals, but mostly on the ligand pathway, is also enhanced, but to a much smaller extent. The intrasite exchange integral $K$ remains unaltered with respect to $Ni_3$ since the magnetic centers are kept unchanged, emphasizing that $K$ is a local, mainly atomic parameter. The raise of the $\sigma$ hopping integral considerably increases $\lambda$ to 13.8 $cm^{-1}$, although its progression is somewhat slowed by the very large $U$ (31 954 $cm^{-1}$). To summarize, considering the rise of the total $J_{eff}$ by a factor close to 3 and the significant degradation of the Heisenberg model for the heterometallic complex, the role played by the diamagnetic central metal can be eventually qualified as *noninnocent*.

***2. Pd$_3$(dpa)$_4$Cl$_2$.*** For this compound, a previous DFT study carried out with the B3LYP functional and based upon Noodleman's standard broken symmetry approach assuming the validity of the Heisenberg model yielded a large coupling constant of 1393 $cm^{-1}$.[60] While carrying out the calculations for $Pd_3$ with the B3LYP functional, we encountered additional problems, namely, the $D^1D^0$ broken symmetry solution, with $M_{s,tot.} = 1$, appears to be more stable than the $D^1D^1$ quintet state, in clear violation of Hund's rule. Such a behavior suggests an *intermediate regime* between the strong antiferromagnetic coupling of the unpaired $\sigma$ electrons and a delocalized 4-electron/3-center $\sigma$ bond. The correct ordering between the $D^1D^1$ and the $D^1D^0$ solutions have been addressed by a slight increase from 20 to 25% of the exact Fock exchange introduced in the hybrid functional, which do not alter significantly the relative energies of the other solutions. So, the parameters for $Pd_3$ shown in Table 5 have been computed with a 25% Fock exchange allowing us to complete the study. The present results show that both hopping integrals in the tripalladium complex increase sharply with respect to NiPdNi and, a fortiori, to $Ni_3$. Such a strengthening of the couplings is not unexpected since the atomic orbitals at the origin of the magnetic interaction are now diffuse 4d. This explains why the $\delta$ interaction, almost unaltered from $Ni_3$ to NiPdNi, is notably enhanced in $Pd_3$, due to an increase of both the $Pd_{terminal}$−N and direct Pd−Pd overlaps. Another change of major importance with respect to NiMNi compounds is the collapse of the $K$ value from ∼5000 to 1960 $cm^{-1}$, which implies a much looser correlation between the unpaired electrons on $Pd^{2+}$, leading to a less tight application of the Hund principle.[61] As a consequence, the non-Hund local singlet configuration ($D^0$) appears energetically affordable in this case. As discussed in a

previous work,[4] a local $D^0$ configuration combined with a triplet on the opposite center can provide a significant stabilizing contribution to the molecular triplet wave functions and lower their energy so as to put them in competition with the pure ($D^1D^1$) state. The discrepancy with respect to the standard model is illustrated by the very different values of $J = 1323$ cm$^{-1}$[60] and $J_{eff} = 2040$ cm$^{-1}$ and by the exceedingly large contribution from the biquadratic exchange ($\lambda = 498$ cm$^{-1}$). Since $\lambda$ can be approximated by the term $(t_\sigma)^4/KU^2$ when $t_\sigma$ remains largely dominant, the decrease of $K$ indeed contributes to the important deviation from the Heisenberg model evidenced from the parameters computed for $Pd_3$. However, the factor most important in determining the magnitude of $\lambda$ remains the $\sigma$ hopping integral, which appears at the fourth power and whose value is three times that of $Ni_3$ and still increased by more than 50% with respect to NiPdNi. Finally, it is worth pointing out that the *effective* magnetic coupling computed for $Pd_3$ is still significantly larger than the one resulting from a standard application of the broken symmetry strategy. Therefore, any attempt to extract magnetic interaction parameters for complexes with $S = 1$ magnetic centers involving 4d orbitals should consider a model Hamiltonian including terms beyond the standard bilinear interactions.

## Conclusions

The main issue of the present work concerns the relationship between the physicochemical nature of magnetic centers with $S = 1$ and the isotropic deviations from the Heisenberg model Hamiltonian. The use of the standard Heisenberg Hamiltonian for the well-documented $Ni_3(dpa)_4Cl_2$ system appears as a correct approximation, as indicated by the small value of $\lambda$ obtained from density functional calculations. The reliability of the DFT/B3LYP methodology in such compounds with $Ni^{2+}$ magnetic centers has been further tested and validated from a comparison with ab initio DDCI results carried out on the smaller model system $[Ni_2(napy)_4Cl_2]^{2+}$. Conversely, systems for which the unpaired electrons are hosted in more diffuse 4d orbitals most probably require a model Hamiltonian including biquadratic interactions. The three-body interactions would probably play an important role too in complexes displaying more than two magnetic centers with 4d orbitals. Along the series of three $MM'M(dpa)_4Cl_2$ complexes investigated in the present work, the $\sigma$ coupling was always found to be largely dominant, especially for the mixed-metal complex. The biquadratic correction $\lambda$ to the Heisenberg Hamiltonian was shown to increase with the substitution of Ni by Pd first in the central position and then, more dramatically, in the terminal ones. Since $\lambda$ approximately varies as $(t_\sigma)^4/KU^2$ as long as the $\sigma$ coupling represents more than 90% of $J$, the importance of the deviation to the Heisenberg model should be correlated first to the increase in the $\sigma$ hopping integral induced by the diffuse 4d orbitals of Pd.

The role of the intrasite exchange integral $K$ between metal atoms of the first and second transition metal series should not be underestimated, however. This parameter, which should be considered as an atomic property of the magnetic center, is related to the energy difference between the local high-spin state and the first excited non-Hund state. For many transition metal atoms with 3d valence shell such as Ni, the order of magnitude of $K$ is large enough ($\sim$5500 cm$^{-1}$ with B3LYP) to exclude any significant interaction between the triplet ground state and the lowest singlet. However, large atoms with more diffuse 4d orbitals such as Pd feature much smaller $K$ values ($\sim$1950 cm$^{-1}$), which contribute to impairment of the quality of the Heisenberg model.

**Acknowledgment.** This work was supported by the Spanish MICINN (Grant CTQ2008-06644-C02-01/BQU) and by the Generalitat de Catalunya (Grant 2009SGR-00462). X.L. thanks the Ramón y Cajal program (Grant RYC-2008-02493).

**Supporting Information Available:** Table for a comparison of the electronic parameters for $Ni_3(dpa)_4Cl_2$ computed with the B3LYP and PBE0 density functionals at the B3LYP-optimized and the X-ray geometries. This material is available free of charge via the Internet at http://pubs.acs.org.

## References and Notes

(1) (a) Dirac, P. A. M. *Proc. R. Soc. London, Ser. A* **1926**, *112*, 661. 1929, *123*, 714. (b) Heisenberg, W. *Z. Phys.* **1926**, *38*, 411. (c) van Vleck, J. H., *Theory of Electric and Magnetic Susceptibilities*; Oxford University Press: London, 1932.

(2) Kahn, O., *Molecular Magnetism*; Wiley-VCH: New York, 1993.

(3) $S = 1$ indicates the maximum spin momentum of one magnetic center.

(4) Bastardis, R.; Guihéry, N.; de Graaf, C. *J. Chem. Phys.* **2008**, *129*, 104102.

(5) Boca, R., *Theoretical Foundations of Molecular Magnetism*; Elsevier: Amsterdam, 1999.

(6) Maurice, R.; Guihéry, N.; Bastardis, R.; de Graaf, C. *J. Chem. Theory Comput.* **2010**, *6*, 55.

(7) Hubbard, J. *Proc. R. Soc. London, Ser. A* **1963**, *276*, 238.

(8) Moreira, I. de P. R.; Suaud, N.; Guihéry, N.; Malrieu, J. P.; Caballol, R.; Bofill, J. M.; Illas, F. *Phys. Rev. B* **2002**, *66*, 134430.

(9) Bastardis, R.; Guihéry, N.; de Graaf, C. *Phys. Rev. B* **2007**, *76*, 132412.

(10) Labèguerie, P.; Boilleau, C.; Bastardis, R.; Suaud, N.; Guihéry, N.; Malrieu, J. P. *J. Chem. Phys.* **2008**, *129*, 154110.

(11) Bera, J. K.; Dunbar, K. R. *Angew. Chem., Int. Ed.* **2002**, *41*, 4453.

(12) Clérac, R.; Cotton, F. A.; Dunbar, K. R.; Murillo, C. A.; Pascual, I.; Wang, X. *Inorg. Chem.* **1999**, *38*, 2655.

(13) Berry, J. F.; Cotton, F. A.; Daniels, L. M.; Murillo, C. A.; Wang, X. *Inorg. Chem.* **2003**, *42*, 2418.

(14) Berry, J. F.; Cotton, F. A.; Lei, P.; Lu, T.; Murillo, C. A. *Inorg. Chem.* **2003**, *42*, 3534.

(15) Berry, J. F.; Cotton, F. A.; Lu, T.; Murillo, C. A.; Wang, X. *Inorg. Chem.* **2003**, *42*, 3595.

(16) Berry, J. F.; Cotton, F. A.; Daniels, L. M.; Murillo, C. A. *J. Am. Chem. Soc.* **2002**, *124*, 3212.

(17) Berry, J. F.; Cotton, F. A.; Lu, T.; Murillo, C. A. *Inorg. Chem.* **2003**, *42*, 4425.

(18) Liu, I. P.-C.; Wang, W.-Z.; Peng, S.-M. *Chem. Commun. (Cambridge, U. K.)* **2009**, 4323.

(19) Wang, C.-C.; Lo, W.-C.; Chou, C.-C.; Lee, G.-H.; Chen, J.-M.; Peng, S.-M. *Inorg. Chem.* **1998**, *37*, 4059.

(20) Lai, S.-Y.; Lin, T.-W.; Chen, Y.-H.; Wang, C.-C.; Lee, G.-H.; Yang, M.-h.; Leung, M.-k.; Peng, S.-M. *J. Am. Chem. Soc.* **1999**, *121*, 250.

(21) Lin, S.-Y.; Chen, I-W. P.; Chen, C.; Hsieh, M.-H.; Yeh, C.-Y.; Lin, T.-W.; Chen, Y.-H.; Peng, S.-M, *J. Phys. Chem. B* **2004**, *108*, 959.

(22) Huang, M.-Y.; Yeh, C.-Y.; Lee, G.-H.; Peng, S.-M. *Dalton Trans.* **2006**, 5683.

(23) Liu, I. P.-C.; Chen, C.-F.; Hua, S.-A.; Chen, C.-H.; Wang, H.-T.; Lee, G.-H.; Peng, S.-M. *Dalton Trans.* **2009**, 3571.

(24) Wagaw, S.; Buchwald, S. L. *J. Org. Chem.* **1996**, *61*, 7240.

(25) Miralles, J.; Daudey, J. P.; Caballol, R. *Chem. Phys. Lett.* **1992**, *198*, 555.

(26) Miralles, J.; Castell, O.; Caballol, R.; Malrieu, J. P. *Chem. Phys.* **1993**, *172*, 33.

(27) Castell, O.; Caballol, R. *Inorg. Chem.* **1999**, *38*, 668.

(28) Moreira, I. de P. R.; Illas, F.; Calzado, C. J.; Sanz, J. F.; Malrieu, J.-P.; Ben Amor, N.; Maynau, D. *Phys. Rev. B* **1999**, *59*, 6593.

(29) Calzado, C. J.; Evangelisti, S.; Maynau, D. *J. Phys. Chem. A* **2003**, *107*, 7581.

(30) Dai, D.; Whangbo, M. H. *J. Chem. Phys.* **2001**, *114*, 2887.

(31) Dai, D.; Whangbo, M. H. *J. Chem. Phys.* **2003**, *118*, 29.

(32) Barone, V.; Cacelli, I.; Cimino, P.; Ferretti, A.; Monti, S.; Prampolini, G. *J. Phys. Chem. A* **2009**, *113*, 15150.

(33) Ruiz, E.; Alemany, P.; Alvarez, S.; Cano, J. *J. Am. Chem. Soc.* **1997**, *119*, 1297.

(34) Bencini, A.; Totti, F.; Daul, C. A.; Doclo, K.; Fantucci, P.; Barone, V. *Inorg. Chem.* **1997**, *36*, 5022.

(35) Nair, N. N.; Schreiner, E.; Pollet, R.; Staemmler, V.; Marx, D. *J. Chem. Theory Comput.* **2008**, *4*, 1174.

(36) Ruiz, E.; Alvarez, S.; Cano, J.; Polo, V. *J. Chem. Phys.* **2005**, *123*, 164110.

(37) Ruiz, E.; Cano, J.; Alvarez, S.; Alemany, P. *J. Comput. Chem.* **1999**, *20*, 1391.

(38) This corresponds to method B in ref 10.

(39) *Gaussian 03*, Revision B 05; Gaussian: Pittsburgh, PA, 2003.

(40) (a) Perdew, J. P.; Burke, K.; Ernzerhof, M. *Phys. Rev. Lett.* **1996**, *77*, 3865. (b) Perdew, J. P.; Burke, K.; Ernzerhof, M. *Phys. Rev. Lett.* **1997**, *78*, 1396. (c) Adamo, C.; Barone, V. *J. Chem. Phys.* **1999**, *110*, 6158.

(41) The DFT optimized Ni−Ni distances are somewhat overestimated, leading to smaller *J* values.

(42) Calzado, C. J.; Cabrero, J.; Malrieu, J. P.; Caballol, R. *J. Chem. Phys.* **2002**, *116*, 2728.

(43) MOLCAS Version 7.0. Department of Theoretical Chemistry, University of Lund: Karlström, G.; Lindh, R.; Malmqvist, P.-Å; Roos, B. O.; Ryde, U.; Veryazov, V.; Widmark, P.-O.; Cossi, M.; Schimmelpfennig, B.; Neogrady, P; Seijo, L *Comput. Mater. Sci.* **2003**, *28*, 222.

(44) (a) Roos, B. O.; Lindh, R.; Malmqvist, P.-Å.; Veryazov, V; Widmark, P.-O. *J. Phys. Chem. A* **2005**, *109*, 6575. (b) Roos, B. O.; Lindh, R.; Malmqvist, P.-Å.; Veryazov, V.; Widmark, P.-O. *J. Phys. Chem. A* **2004**, *108*, 2851.

(45) Calzado, C. J.; Malrieu, J. P.; Cabrero, J.; Caballol, R. *J. Phys. Chem. A* **2000**, *104*, 11636.

(46) Barone, V.; Cacelli, I.; Ferretti, A.; Prampolini, G. *J. Chem. Phys.* **2009**, *131*, 224103.

(47) (a) CASDI program: Benamor, N.; Maynau, D. *Chem. Phys. Lett.* **1998**, *286*, 211. (b) Maynau, D.; Benamor, N.; Pitarch-Ruiz, J. *CASDI Program*; Laboratoire de Chimie et de Physique Quantiques, Toulouse University: Toulouse, France, 1999.

(48) Broer, R.; Maaskant, W. J. A. *Chem. Phys.* **1986**, *102*, 103.

(49) Tabookht, Z.; López, X.; de Graaf, C. *J. Phys. Chem. A* **2010**, *114*, 2028.

(50) Aduldecha, S.; Hathaway, B. *J. Chem. Soc., Dalton Trans.* **1991**, 993.

(51) Kiehl, P.; Rohmer, M. M.; Bénard, M. *Inorg. Chem.* **2004**, *43*, 3151.

(52) Peng, S. M.; Wang, C. C.; Jang, Y. L.; Chen, Y. H.; Li, F. Y.; Mou, C. Y.; Leung, M. K. *J. Magn. Magn. Mater.* **2000**, *209*, 80.

(53) Kitagawa, Y.; Shoji, M.; Koizumi, K.; Kawakami, T.; Okumura, M.; Yamaguchi, K. *Polyhedron* **2005**, *24*, 2751.

(54) Liu, I. P.-C.; Bénard, M.; Hasanov, H.; Chen, I.-W. P.; Tseng, W. H.; Fu, M. D.; Rohmer, M. M.; Chen, C. H.; Lee, G. H.; Peng, S. M. *Chem.—Eur. J.* **2007**, *13*, 8667.

(55) Theoretical work is in progress analyzing the underestimation of the computed *J* in $Ni_3$ and $Ni_5$ EMAC systems, both containing two $S = 1$ centers.

(56) Becke, A. *J. Chem. Phys.* **2000**, *112*, 4020.

(57) Chermette, H.; Ciofini, I.; Mariotti, F.; Daul, C. *J. Chem. Phys.* **2001**, *114*, 1447.

(58) Ciofini, I.; Adamo, C.; Chermette, H. *Chem. Phys.* **2005**, *309*, 67.

(59) Ciofini, I.; Chermette, H.; Adamo, C. *Chem. Phys. Lett.* **2003**, *380*, 12.

(60) López, X.; Rohmer, X.; M. M.; Bénard, M. *J. Mol. Struct.* **2008**, *890*, 18.

(61) This fact might explain the difficulties encountered to get a correct ordering of the $D_1D^1$ and $D_1D^0$ states.

JP106038W